Russian Geology and Geophysics © 2020, V.S. Sobolev IGM, Siberian Branch of the RAS
Vol. 61, No. 1, pp. 68–78, 2020 *DOI:10.15372/RGG2019079* *Geologiya i Geofizika*

Evolution of the Sedimentary Basin of the Continental Margin of Antarctica in the Cooperation Sea (from Results of Numerical Modeling)

G.L. Leitchenkov[a,b,] ✉, Yu.I. Galushkin[c], Yu.B. Guseva[d], E.P. Dubinin[c]

[a]*I.S. Gramberg All-Russia Scientific Research Institute for Geology and Mineral Resources of the Ocean, Angliiskii pr. 1, St. Petersburg, 190121, Russia*

[b]*St. Petersburg State University, Institute of Earth Sciences, Universitetskaya nab. 7–9, St. Petersburg, 199034, Russia*

[c]*Lomonosov Moscow State University, Earth Science Museum, Leninskie Gory 1, Moscow, 119991, Russia*

[d]*Polar Marine Geosurvey Expedition, ul. Pobedy 24, St. Petersburg, Lomonosov, 198412, Russia*

Received 24 April 2018; received in revised form 27 July 2018; accepted 17 September 2018

Abstract—We discuss the structure of the Earth's crust the seismic stratigraphy, thermal evolution, and stretching of the lithosphere in the sedimentary basin of the Cooperation Sea located on the continental margin of Antarctica in the south of the Indian Ocean. The sedimentary basin includes intracontinental and marginal rifts; the former is located on the shelf, and the latter, in the deep-water area. A seismostratigraphic analysis has revealed four sequences in the sedimentary cover of the intracontinental rift, which formed from middle Permian to late Cenozoic, and nine sequences in the sedimentary cover of the marginal rift, which have been deposited since the Middle Jurassic. One-dimensional numerical modeling of the thermal regime and the basement subsidence was performed over 18 points along the profile crossing the basin from the shelf to the lower continental rise. Based on the results of modeling and seismostratigraphic analysis, we have established variations in rock temperature with depth and in the degree of lithosphere stretching throughout the basin rift history. The modeling showed that the depth of the basement subsidence and the thickness of the crystalline part of the basin crust are governed by the lithosphere stretching before sedimentation. The maximum stretching is reached at the depocenters of rift structures (where the crust is the thinnest), being 2.8 before sedimentation and 1.16 after it in the intracontinental rift and 4.6 and 1.4, respectively, in the marginal rift.

Keywords: continental margin, sedimentary basin, rifting, numerical modeling of basins, lithosphere stretching, Antarctica, Cooperation Sea

INTRODUCTION

The Cooperation Sea is located in the southern (Antarctic) part of the Indian Ocean between 55° E and 80° E, occupying the area between the continental shelf and the abyssal plain (Fig. 1). The western part of the Cooperation Sea shelf is relatively narrow, its width varying from 50 to 100 km, while the eastern one runs into the continent for more than 300 km and is known as the Prydz Bay. The continental slope and rise range in depth from 450–500 to 4200–4500 m and extend 420–450 km into the ocean, being one the widest margin of Antarctica. The Cooperation Sea contains a large sedimentary basin that formed as the result of rifting and the breakup of East Gondwana (separation of Indian and Antarctica (Leitchenkov et al., 2014)). The basin extends to the west into the Cosmonaut Sea, and to the east into the Davis Sea (Fig. 1).

✉ Corresponding author.
E-mail adress: german_l@mail.ru (G.L. Leitchenkov)

The objective of the presented study was numerical modeling of the thermal evolution of the lithosphere underlying the basin, the history of its basement subsidence and the estimation of lithospheric stretching during the rift phase. The modeling was performed based on the geophysical data obtained in the Cooperation Sea by the Polar Marine Geosurvey Expedition (PMGE) during the 52nd and 57th Russian Arctic Expeditions (RAE) in 2007 and 2012, respectively and the results of their interpretation (seismic stratigraphy analysis and crustal thickness estimation).

The results of the performed modeling in combination with the estimation of the crustal thickness allow us to suppose that at the early stage of rifting, before the start of rift-related sedimentation, the lithosphere might have had quite a high stretching amplitude. Data on sedimentary thicknesses and assumption about the sea bottom deepening make it possible to estimate the total amplitude of the lithospheric stretching during the rifting.

For this purpose, in our study, we applied analysis of the basin's tectonic subsidence in the assumption of the local

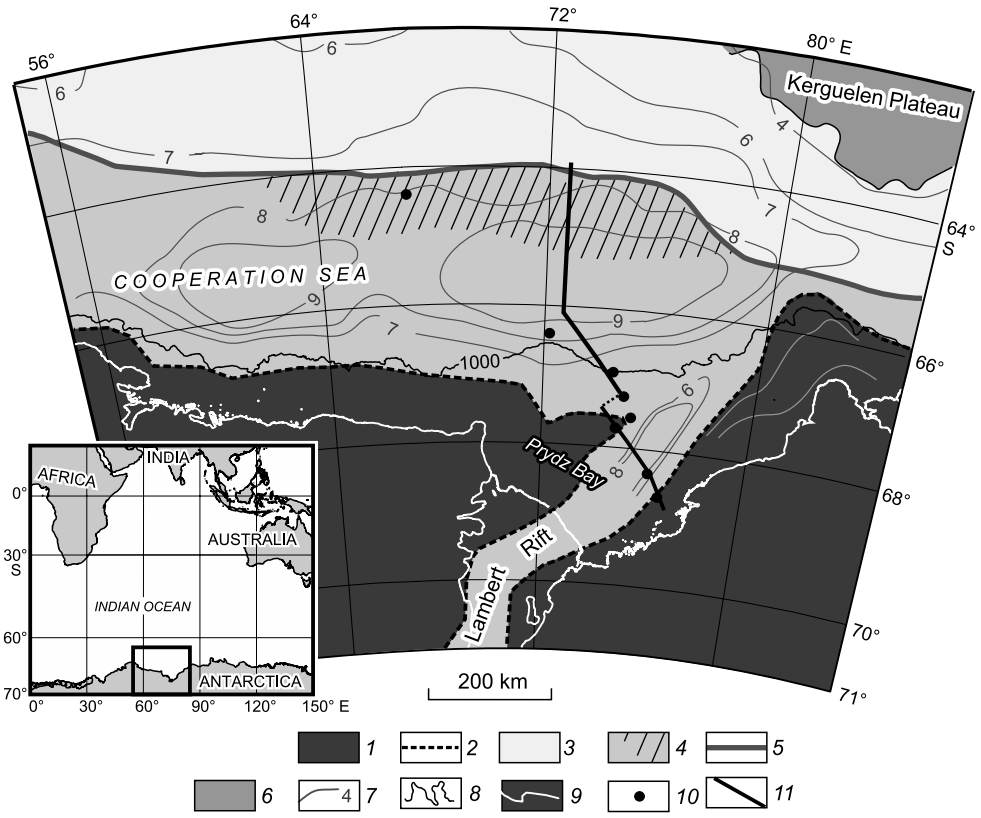

Fig. 1. Tectonic structure of the Cooperation Sea Basin from (Leitchenkov et al., 2010 with changes and additions). *1*, crystalline shield; *2*, boundary between the crystalline shield and the sedimentary basin; *3*, intracontinental and marginal rifts; *4*, zone of mantle exhumation; *5*, continent-to-ocean boundary; *6*, volcanic plateau; *7*, depth to the basement (km); *8*, 1000 m isobaths; *9*, coastal line and ice shelf boundaries; *10*, ODP boreholes; *11*, Reflection and refraction seismic profile providing information about the crustal structure and sedimentary cover to be used in numerical modeling.

isostatic rebound of the lithosphere to changes in surface (sediments and water) and inner (rock densities within the lithosphere) loads.

THE REGION'S GEOPHYSICAL RESEARCH AND A SHORT OVERVIEW OF ITS GEOLOGICAL HISTORY

A first geophysical study in the Cooperation Sea was conducted in 1981 by an Australian expedition (Stagg, 1985). Since then multiple surveys have been carried out by groups from Australia, Germany, Russia, and Japan (Leitchenkov et al., 2014). A typical survey normally included multichannel seismic, gravity and magnetic observations. In 1988 and 2000, 5 boreholes in the Prydz Bay shelf and 2 boreholes in the upper continental rise were drilled by ODP (Legs 119 and 188) (Barron and Larson, 1991; Cooper et al., 2004).

In 2007, a joint Russian–German expedition carried out a study during the 3d International Polar Year (IPY) (Project "History of Geodynamic Development, Sedimentation and Environmental Changes in Cooperation Sea Basin and Southern Kerguelen Plateau") (Leitchenkov et al., 2010). Multichannel seismic and refraction seismic data were collected under this project along a line crossing the continental rise and the abyssal plain from south to north. The survey provided reliable data on the crustal thickness and the structure of sedimentary cover. In 2012, PMGE extended the 2007 profile to the Prydz Bay shelf, so it crossed the main tectonic structures of the Cooperation Sea.

Integration and interpretation of all available geophysical data enabled us to conclude that the Prydz Bay shelf includes the northern termination of an extended intracontinental rift known as Lambert Rift (Leitchenkov et al., 2014). Within the outer shelf, it meets the marginal rift to form a triple junction.

The geological data collected in the coastal area demonstrate that the Lambert Rift started to form in the late Carboniferous. It is confirmed by the significant denudation of the Earth's surface, indicating the thermal uplift of the lithosphere in the rims of the forming rift (Lisker et al., 2003) as well as by magmatism manifestations such as intrusion of dolerite dikes and olivine–leucite basalts flows of this age (Leitchenkov et al., 2014). The further development of the Lambert Rift is documented by the formation of the Perm-

ian–Triassic terrigenous coal-bearing deposits 2 km thick that were found in the western rim of the Lambert Rift (Aleksashin and Laiba, 1993). The presence of stretching at that time is confirmed by the intrusion of Early Triassic dolerite dikes (Mikhalsky and Sheraton, 1993). The Paleozoic–early Mesozoic phase of rifting ended with a short period of relative stabilization that covered the time from the Late Triassic to the beginning of the Middle Jurassic (about 170 Ma). This was followed by another stage of tectonic activity with repeated stretching of the intracontinental rift and formation of an extended rift zone between India and Antarctica (Truswell et al., 1999; Leitchenkov et al., 2014). The end of rifting and the lithosphere's break-up is thought to have occurred at 140–130 Ma. This age is suggested from the oldest magnetic anomalies identified in the Cooperation Sea (Leitchenkov et al., 2010).

THE STRUCTURE OF EARTH'S CRUST AND SEDIMENTARY COVER OF THE CONTINENTAL MARGIN IN THE COOPERATION SEA

The structure of the Earth's crust was studied by gravity modeling (using GM-SYS 4.8 software) with use of seismic reflection and refraction data. The basement surface and seismic horizons interpreted from reflection seismics were recorded during gravity modeling (Fig. 2).

According to gravity modeling, the crustal thickness in the coastal area varies from 30 to 35 km and is significantly reduced in the axial part of the Lambert Rift in the Prydz Bay where the crystalline basement deepens down to 12 km, while the Moho discontinuity rises to 22 km (Fig. 2). The crust of the rift flanks on the shelf is 25–26 km thick. Under the continental slope, upper continental rise and lower continental rise, the crustal thickness is reduced to 15, 10 and 5 km, respectively (Fig. 2).

The outer part of the marginal rift (between 450 and 570 km) forms a transitional crust with mantle exhumation (Figs. 1, 2) (Leitchenkov et al., 2010, 2014). A mantle exhumation is a rupture in lithosphere formed due to its extreme stretching during the final stage of rifting when the upper mantle rises and is actually outcropped in the sea floor (Boillot and Froitzheim, 2001). Such processes are typical for nonvolcanic margins and have been well studied in the northern part of the Atlantic Ocean (Boillot and Froitzheim, 2001) and in the southeastern part of the Indian Ocean (Leitchenkov et al., 2014). Due to the uplift, mantle rocks (peridotites) undergo serpentinization, changing their composition, so the values of their density and seismic velocities are significantly reduced.

The presence of the exhumed mantle in the marginal rift is confirmed by the increased thickness of the crystalline crust that cannot be explained by progressing stretching; by its average density (Fig. 2); by the presence of high-amplitude uplifts of the basement that are typical for peridotite ridges; and by the complex crustal structure in seismic re-

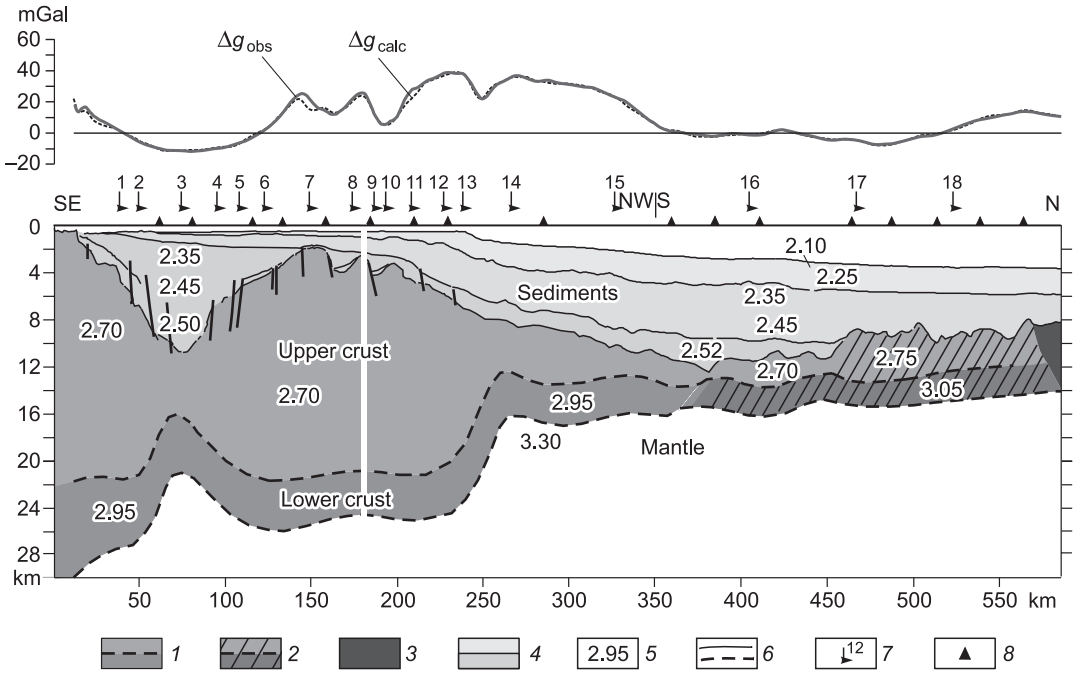

Fig. 2. Crustal model across the Prydz Bay shelf and deep-water part of the Cooperation Sea. *1–3*: crystalline crust: *1*, continental; *2*, transitional (composed of mainly serpentinized peridotites); *3*, oceanic; *4*, sedimentary cover (the color marks rift and post-rift deposits); *5*, rock density (g/cm^3); *6*, seismic and/or density boundaries; *7*, pseudowells (their numbers are indicated on top); *8*, seismic refraction points. See Fig. 1 for profile location.

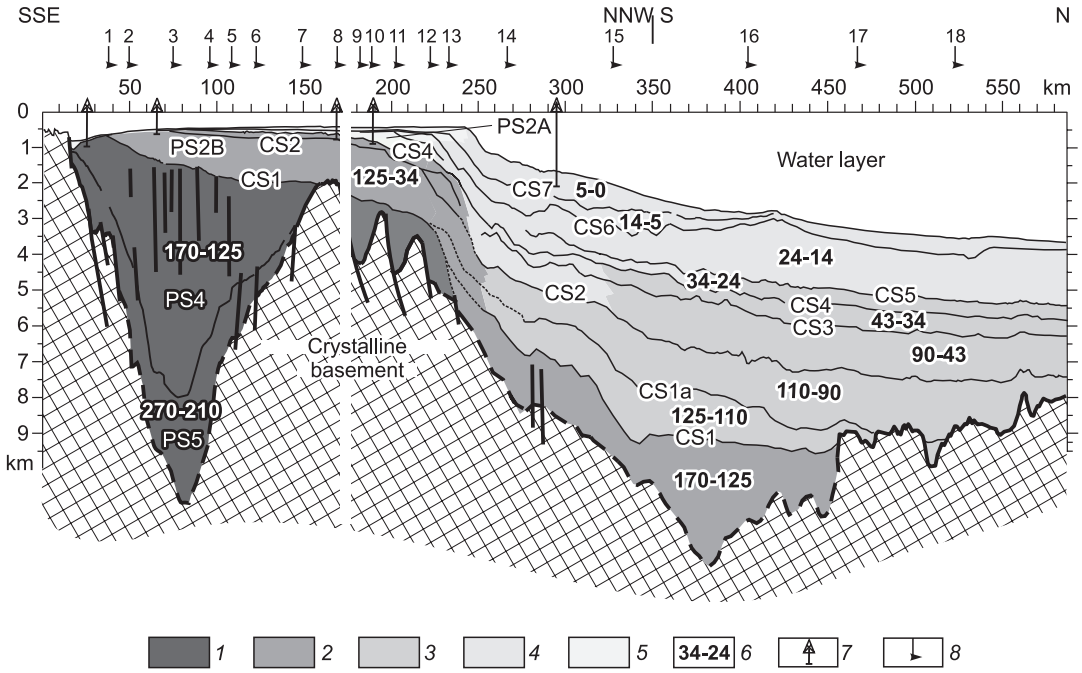

Fig. 3. Interpretive seismic section across the continental margin in the Cooperation Sea. *1–5*: lithology: *1*, conglomerates, sandstones, siltstones, mudstones, coals (alluvial, lacustrine, lagoonal); *2*, argillites and siltstones (continental and shallow marine); *3*, argillites, clays (hemipelagic deposits); *4*, clays and silts/siltstone (levee deposits, debris flows deposits, landslides); *5*, diamictites (glacial-fluvial and glacial-marine); *6*, age (in Ma) of seismic sequences; *7*, ODP drill-holes, *8*, pseudowells (their numbers are indicated on top) used in modeling. CS1, CS1a, CS2, CS3, CS4, CS5, CS6, CS7, seismic horizons; PS5, PS4, PS2B, PS2A, seismic sequences in the Prydz Bay shelf. The basement surface marked with the solid line is derived from multichannel seismic data. The basement surface marked with the dashed line is derived from seismic refraction data. See Fig. 1 for profile location.

cords showing multiple diffractions and discontinuous reflectors that are characteristic for different degrees of serpentinized mantle (Leitchenkov et al., 2010). In addition, a zone of mantle exhumation has been discovered on the conjugate continental margin of India (Mangipudi et al., 2014).

The seismic and drilling data allow us to identify seismic sequences in the sedimentary cover of the Cooperation Sea basin and to determine their ages. The sedimentary cover is subdivided into two major units corresponding, respectively, to the syn-rift and post-rift phases of deposition (Fig. 3). Multichannel seismic reflection data enable recognizing the crystalline basement for the most part of the basin, excluding only the central part of the intracontinental rift and the inner part of the margin rift, where, however, it can be determined using the refraction seismic data.

The seismic stratigraphy model for the sedimentary cover of the Prydz Bay shelf was suggested by Stagg (1985) based on an Australian seismic survey conducted in 1981 and was later specified using ODP drilling data and the results obtained by the Soviet and Russian expeditions of 1986–1988 and 2012. According to this model, the sedimentary cover of this area is divided into four seismic sequences: PS5, PS4, PS2B and PS2A (three upper ones were sampled by the ODP drilling (Barron and Larson, 1991; Cooper et al., 2004)).

The lower sequence PS5 is characterized by high seismic velocities: 4.8–5.0 km/s and its thickness reaches 4.5 km (Fig. 2). This sequence was not sampled by drilling, but considering its high seismic velocities (4.5–5.0 km/s), it might be composed of the Permian–Triassic deposits analogous to those found on the western flank of the Lambert Rift (Leitchenkov et al., 2010).

Sequence PS4 reaches its maximum thickness (3.5–4.0 km) in the axial part of the rift and is limited in its top by an angular unconformity (Fig. 3). According to the drilling data, it is composed of siltstones and thin layers of sandstones (Barron and Larson, 1991). This sequence has been sampled by drilling but its age has not been determined due to absence of fossils. Based on structural characteristics of PS4 (Fig. 3), we suggest that it was deposited during the final rifting stage during the Late Jurassic–Early Cretaceous.

Sequence PS2B covers the most part of the Prydz Bay shelf. The drilling data show that it is mainly composed of sandstones and siltstones with carbonized vegetative matter (Barron and Larson, 1991). The sediments in the sampled (upper) part of the sequence were deposited in the cold moist climate of the Early Cretaceous.

The upper sequence PS2A spreads over the area from the middle shelf to the continental slope, has a progradational pattern and was sampled by four ODP holes (Fig. 3). Its basal part penetrated by well 1166 is composed of the middle and late Eocene sandstones deposited in fluvial conditions and lagoons in cold moist climate near the glacier margin (Cooper et al., 2004). The remaining part of the section

formed during the early-late Oligocene and includes massive and stratified diamictites of glacial and glacial-marine origin (Barron and Larson, 1991).

The seismic stratigraphy model for the deep-water basins of East Antarctica was developed by Russian scientists after many years of extensive research (Leitchenkov et al., 2007). Based on this model, nine seismic horizons CS1, CS1a, CS2, CS3, CS4, CS5, CS5a, CS6 and CS7 were identified in the sedimentary cover of the Cooperation Sea, a part of them were correlated with horizons (sequence boundaries) recognized in the Prydz Bay shelf (Fig. 3).

Horizon CS1 forms the top of the rift unit filling the regional through of the marginal rift and the local structures of the stretching (half-grabens). Its age corresponds to the beginning of sea floor spreading in the Cooperation Sea and varies from 130 to 125 Ma. The rift unit formed in continental and shallow marine conditions, so it is mainly composed of sandstone and siltstones.

Horizon CS1a is traced in the middle and lower continental rise. Its formation is probably related to the changes in depositional environments influenced by intensive volcanism in the southern part of the Kerguelen Plateau between 120 and 110 Ma and by the Indian Ocean development. The underlying sedimentary sequence (between horizons CS1 and CS1a) deposited at the early stage of oceanic development and may be composed of mainly siltstones and mudstones. All overlying sequences are predominantly composed of hemipelagic and pelagic sediments, but may also locally contain coarse-grained deposits formed by gravity flows.

Horizon CS2 is confidently recognized everywhere in the deep-water area of the Cooperation Sea. Its age is considered to be 90–80 Ma corresponding to the gate-way opening and changes in the ocean water circulation in the South Atlantic and Indian Oceans (Lawver et al., 1992; Leitchenkov et al., 2010).

Horizons CS3–CS7 were identified in all the sedimentary basins of the East Antarctic continental margin and are correlated between the basins (Leitchenkov et al., 2007). Horizon CS3 is dated as middle Eocene (48–43 Ma), and this age is based on the horizon's overlapping onto the dated (by magnetic anomalies) oceanic crust.

Horizon CS4 is the most prominent interface in the sedimentary cover almost everywhere on the East Antarctic margin exhibiting a profound change in the seismic reflection pattern. It is widely accepted that this horizon correlates with the onset of large-scale Antarctic glaciation at about 34 Ma (Leitchenkov et al., 2007). The age of CS5, CS6 and CS7 is reliably determined from the ODP drilling (Figs. 1, 3) and corresponds to 24–22, 14–12 and 5–3 Ma, respectively. Formation of horizon CS6 is related to the global cooling that occurred in the end of the middle Miocene and resulted in the stabilization of the Antarctic glaciation and decrease in the rate of sedimentation on the Antarctic continental margin.

ROCK TEMPERATURE FLUCTUATIONS DURING BASIN SUBSIDENCE

The subsidence and rock temperature evolution of the sedimentary basin were reconstructed along the profile crossing the continental margin using the GALO software (Figs. 2, 3) at 18 evenly spread points (pseudowells). The process of modeling using this software was considered in detail in (Galushkin, 2007, 2016), so in this paper only the key elements will be highlighted. The modeling process is based on a numerical solution of the 1D nonstationary equation for heat transfer that accounts for time and depth-related changes in thermophysical rock properties in flat basin approximation when the temperature depends only on the depth and time. The temperatures were calculated for a domain including the sedimentary cover, undelaying the lithosphere, and a part of the asthenosphere to the depths of 80–100 km.

Solving the heat-transfer equation for the domain's upper boundary the temperature was selected to match the climatic conditions at the sea bottom (basin surface) within the considered time period. To determine the paleotemperatures we relied upon (Frakes, 1979) where the author indicates yearly average temperature changes on the Earth's surface in relation to geographical latitudes and geological times for the most part of the Phanerozoic that were specified to correlate with the modern understandings of climate changes in Antarctica (Florido and Siegert, 2009). These surface values were then recalculated to obtain sea floor temperatures considering sea depth changes within the period of basin development.

At the low boundary of the computation domain (*ZM*), whose depth for different pseudowells varied from 84 to 90 km, a constant temperature (TM) was set, its value varying for different parts of the basin in relatively narrow ranges (from 1150 to 1180 °C). The values ZM and TM were determined by the crossing of geotherm T_{cold} (z) with a peridotite solidus curve that is characterized by a low level of H_2O (less than 0.2%) (Wyllie, 1979). In this case, T_{cold} (z) determined the temperature distribution in the basement (excluding sedimentary cover) matching the minimum thermal flow in the history of the basin's development (for more details see (Galushkin, 2007)). In our study, the minimum thermal flow was considered to be equal to 1.1 heat units (hU) or 46 MW/m^2. The differences in the ZM and TM values were due to different degrees of lithospheric thinning during the initial stage marginal deposition in the different parts of the basin.

The GALO software, like any other software packages for numerical modeling (Ungerer et al., 1990; Ungerer, 1993; Welte et al., 1997) utilizes the data on a sedimentation rates changes, erosional processes and hiatuses in deposition. During modeling, GALO calculates changes in porosity in sedimentary rocks (during their cementation) as well as their density, thermal conductivity and capacity, and the degree of their heat generation caused by lithological chang-

es, increased deepening depth and temperature. Moreover, it takes into account the dependence of the thermal conductivity of water and rock matrix on temperature (Galushkin, 2007, 2016).

The process of sedimentary cover formation was modeled as the virtual deposition of the uncompacted sediments forming elementary (no more than 10 m thick) layers of Δz in thickness. The temperature computation included the sedimentary layer, crystalline crust and underlying mantle down to 100 km. Within this domain, the mesh size increased with the depth and comprised about 1 km at a depth of 100 km. The time intervals varied from 400 thous. years for slow sedimentation rates and 16 thous. years for fast ones.

When calculating the thermophysical parameters of the sedimentary rocks, we used the global average values of the petrophysical matrix characteristics of the main lithological units. The lithology was predicted based on the results of seismic stratigraphy analysis.

Figure 4 shows (as an example) changes in rock temperatures for pseudowells 3, 4, 14 and 16, and Fig. 5 demonstrates the modeling results for the sedimentary section. The maximum thicknesses of the sedimentary cover were recorded in the Lambert Rift in the Prydz Bay and under the middle continental rise of the Cooperation Sea (Figs. 3–5). In the Lambert Rift, the maximum sedimentation rates are related to the first (210–170 Ma) and second (170–125 Ma) phases of rifting, and in the marginal rift to the main phase (170–125 Ma) of rifting and the glaciation period (34–0 Ma).

The degree of organic matter (OM) maturation determined through the values of vitrinite reflectance (R^{o}_{Vt}, %) served as an indicator of the integral thermal history of the basin. Figures 4 and 5 demonstrate that the sedimentary

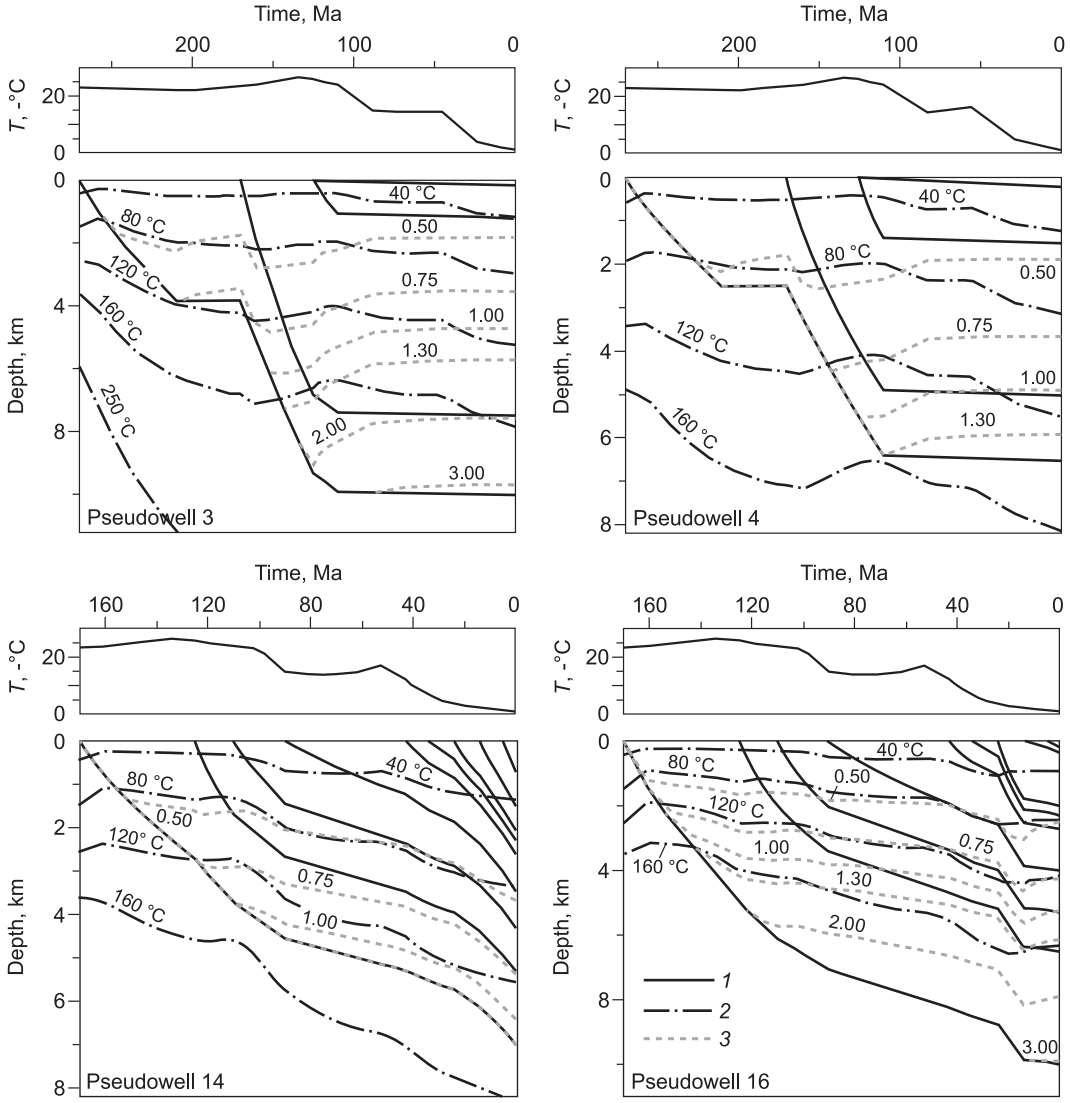

Fig. 4. Temperature and organic matter maturity changes during basin subsidence calculated for pseudowells 3, 4, 14 and 16 (see Figs. 2, 3). The upper parts of the figure demonstrate changes average annual temperature at sea bottom (Frakes, 1979; Florindo and Siegert, 2009). *1*, base of the seismic sequences; *2*, isotherms; *3*, vitrinite reflectance isolines (%).

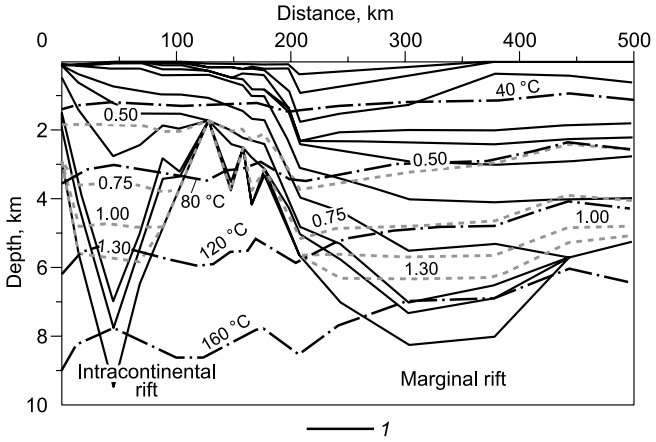

Fig. 5. Calculated vitrinite reflectance and temperature distributions. *1*, seismic horizons. For the rest of the legend see Fig. 4.

rocks of the upper 6 km are of moderate maturity corresponding to the so-called oil generation window ($0.50 \le R^{o}_{Vt} \le 1.30\%$).

CHANGES IN LITHOSPHERIC STRETCHING DEGREE DURING THE RIFT HISTORY OF COOPERATION SEA BASIN

The depth and age of the seismic sequences (Fig. 3) together with suggested sea floor paleodepths (curves 4 in Fig. 6) enabled us to reconstruct the thermal history of the basin and to calculate the variations of its tectonic subsidence, i.e., the subsidence of the basement-surface due to the stretching and thermal cooling of the lithosphere. We assumed that before the start sedimentation, an arch had dominated over the area. Lines 1 (Fig. 6) demonstrate changes in tectonic subsidence, i.e., changes in the depth of basement (ZT_s) calculated after removal of water and sediments load (Galushkin, 2007, 2016; Galushkin et al., 2018) using the following expression:

$$ZT_s(t) - ZT_s(0) = \frac{\rho_a - \rho_s(t)}{\rho_a} \cdot S(t) + \frac{\rho_a - \rho_w}{\rho_a} \cdot [Z_w(t) - Z_w(0)], \quad (1)$$

where t denotes the time; $t = 0$, the starting point of the basin formation; $Z_w(t)$, the paleodepths at time t; $S(t)$, thickness of sediments; ρ_a and ρ_w, the asthenosphere and water densities, respectively. The average density of sedimentary rocks $\rho_s(t)$ at any time moment t of its development was determined as:

$$\rho_s(t) = \frac{\int_0^{S(t)} \rho_s(Z,t) \cdot dZ}{S(t)}. \quad (2)$$

Formula (1) was derived under the assumption of the isostatic response to a load of water and sediments. If sedimentation occurred within the mainland, in (1) we accept $Z_w(t) = 0$. Hence, changes in the tectonic subsidence at the time t relative to the subsidence value at the time of sedimentation onset (sag phase) determined by changes in the weight of the sedimentary column and sea paleodepths within the same time interval. In other words, curves 1 in Fig. 6 correspond to the classical definition of basin subsidence (Parson and Sclater, 1980).

Figure 7 shows thermal conditions of the lithosphere as they were calculated for pseudowell 3 in the intracontinental Lambert Rift and for pseudowell 14 in the marginal rift. In our calculation, we assumed that in the initial period of the basin's development (before lithosphere started to stretch), the thickness of the crustal layers and the thermophysical parameters of lithospheric rocks were similar to the ones of the standard continental lithosphere (Table 1) (Baer, 1981; Galushkin, 2007). It should be noted that the contribution of radiogenic elements of the crystalline crust into the surface heat flow is about 21 MW/m^2 (Table 1), which correlates with the data on the thermophysical properties of the rocks of the Indian crystalline shield adjoining to the studied region before the Gondwana break-up (Gupta et al., 1991).

Since the GALO software calculated temperature distribution not only for the sedimentary cover but also for the underlying lithosphere (Fig. 7), we had an opportunity to use another method for estimation of the amplitudes of the tectonic subsidence (Galushkin, 2007, 2016). This additional method is based on computation of rock density vs. depth both for crystalline crust and for mantle trough the geological time. The corresponding variations of tectonic subsidence were calculated using the formula (Galushkin, 2007, 2016):

$$ZT(t) - ZT(0) = \frac{G(t) - G(0)}{\rho_a \cdot g}. \quad (3)$$

Table 1. Parameters of standard continental lithosphere to be used in modeling

Parameter	Upper crust		Lower crust	Mantle
Basement depth, km	5.0	15.0	36.0	> 36
density, kg/m^3	2750	2750	2900	3300
Thermal conductivity, W/m/K	2.72	2.72	1.88	$K = f(T)$
Thermal generation, μW/m^3	1.465	0.84	0.21	0.004

Note. Dependence of mantle rock thermal conductivity (K) on the temperature was determined using equations (McKenzie et al., 2005), and the lithospheric parameters (Baer, 1981; Galushkin, 2007, 2016).

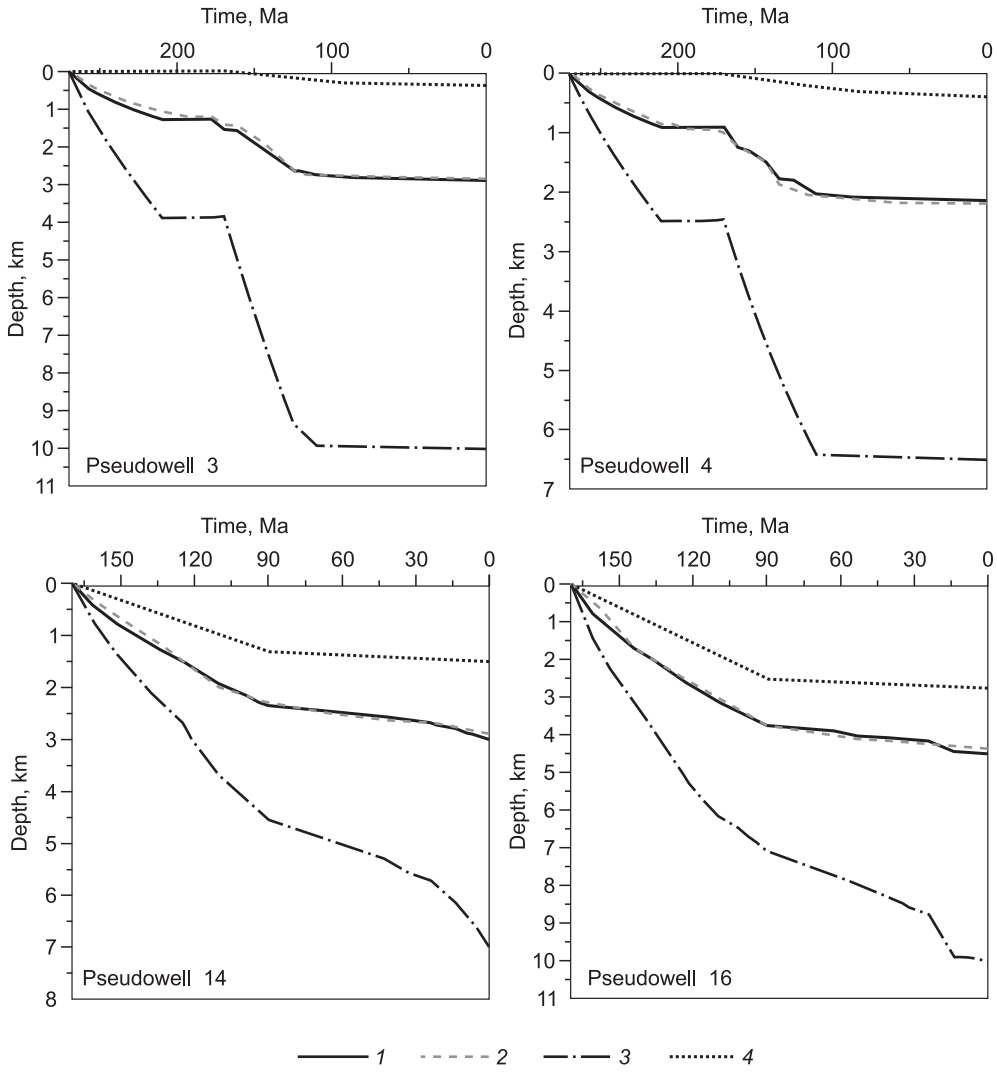

Fig. 6. Tectonic subsidence variations for the Cooperation Sea Basin for pseudowells 3, 4, 14 and 16. The calculations have been performed in the assumption of local isostatic rebound to load. *1*, tectonic subsidence of the basement surface, calculated upon removal of water and sediments load; *2*, tectonic subsidence due to changes in the densities of crystalline consolidated crust and mantle rocks; *3*, changes in thickness of sedimentary cover; *4*, sea paleodepth.

where g denotes the gravity acceleration; G, the weight of the crust and mantle of a certain fixed thickness l_0:

$$G(t) = g \cdot \int_0^{l_0} \rho_l(Z,t) \cdot dZ \ . \quad (4)$$

Here, the basement's rock density $\rho_l(Z, t)$ is the function of temperature $T(Z, t)$, pressure $P(Z, t)$ and time t:

$$\rho_l(Z,t) = \rho_0(Z,t) \cdot [1 - \alpha \cdot T(Z,t) + \beta \cdot P(Z,t)], \quad (5)$$

where $\alpha = 3.2 \times 10^{-5}$ °C^{-1} denotes the thermal coefficient of expansion (Parsons and Sclater, 1977); $\beta = 0.00079$ kbar^{-1}, the isothermal rock compaction coefficient (Touloukian and Ho, 1981); $\rho_0(Z, t)$, the rock density distribution with depth under the standard conditions (P = 1 atm and T = 20 C).

Parameter ρ_0 includes variations of density caused by differences in rock composition; phase transitions within the peridotite mantle as well as lithospheric stretching. The corresponding variations of tectonic deepening (3) can be seen in Fig. 6 (curves 2). According to (5), the temporal fluctuations in distribution of the crustal and mantle rock densities with depth that determine the variations of the tectonic subsidence depend on the changes of temperature, pressure and rock composition with depth as well as on changes in depths of phase transition in the mantle during basin development (Galushkin, 2016). Rock density with depth changes both during lithospheric stretching and during its thermal activation.

As it was mentioned above, this approach was applied in the assumption of local isostatic rebound (Galushkin, 2016; Galushkin et al., 2018). Curves 3 in Fig. 6 show how the

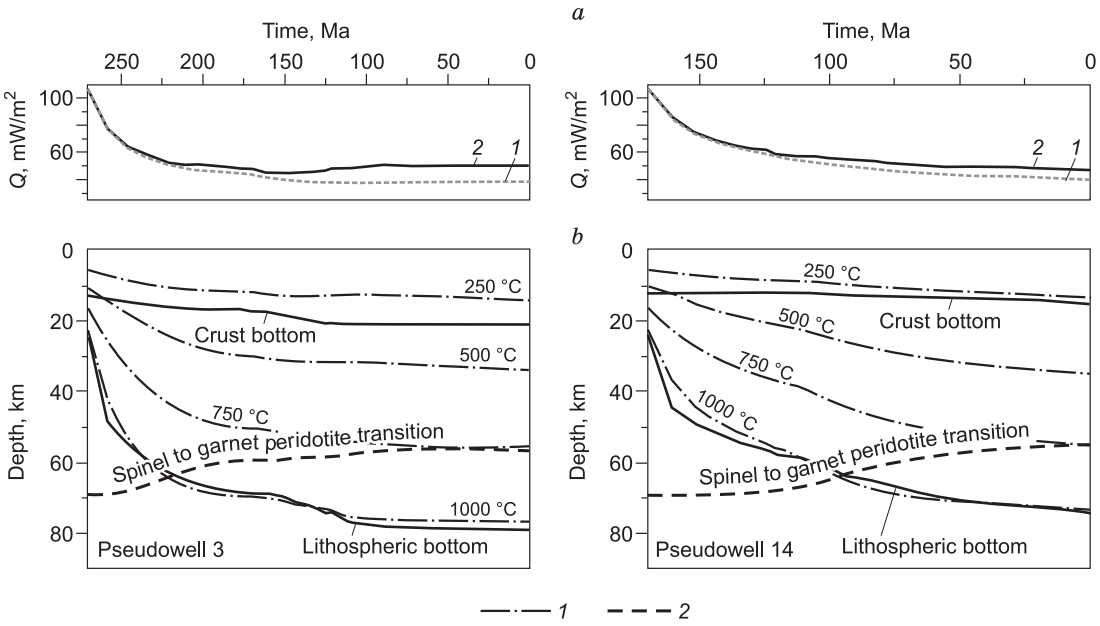

Fig. 7. Thermal history of lithosphere for intracontinental rift (pseudowell 3) and marginal rift (pseudowell 14). *a*, Changes in heat flow: *1*, heat flow through the basement surface; *2*, heat flow through the sedimentary cover; *b*, lithospheric thermal regime evolution: *1*, isotherms (°C) *2*, spinel to garnet peridotite transition depth in the mantle. The figure shows the Moho discontinuity, and the base of lithospheric determined from the crossing of a peridotite solidus curve (water saturation of no more than 0.2%) (Wyllie, 1979) and current isotherm T (Z, t) in the lithosphere.

thickness of the sedimentary cover changes during basin subsidence, and curves 4 in the same depict sea floor depths. Summing 3 and 4 in Fig. 6 results in the total depth of the basement subsidence calculated from the sea surface.

The stretching amplitudes of the lithosphere that were calculated from the profile (Figs. 2, 3) can be seen in Fig. 8*a*. In the beginning of the modeling procedure when the value of the lithosphere presedimentary stretching β_0, amplitude was yet unknown, it was set reasonably but arbitrarily. For this arbitrary value, the thickness of crystalline crust at the time when the sedimentation started was determined as $H_{0sed} = H_0/\beta_0$. The GALO modeling gave us the stretching amplitude for the period of rift formation β_{12}. Then, the summed amplitude of the lithospheric stretching was determined as $\beta_{sum} = \beta_0 \times \beta_{12}$, i.e., the stretching amplitude to ensure the calculated basement subsidence with sediments and water loads taken into account. If β_{sum} was different from $\beta_{0observ}$ (that was derived from the observed thickness of modern consolidated crust H_{observ} in Fig. 2; $\beta_{0observ} = 36/H_{observ}$), the β_0 would be changed, and the procedure would be repeated until β_{sum} became close to $\beta_{0observ}$ in a way the calculated thickness of the crystalline crust (curve 2 in Fig. 8*b*) became close to the value of H_{observ} (curve 1, in Fig. 8*b*). In this way, the results presented in Figs. 4–8 were obtained.

DISCUSSION

Using the GALO package for modeling of the Cooperation Sea sedimentary basin assumed that the basin could be considered as flat, which means temperature and depth changes along the X and Y axes were small relative to those along the Z axis. We consider that the model-based corrections for our estimations of tectonic subsidence were not significant for all the considered territories.

It is noteworthy that the calculated changes in vitrinite reflectance for the sedimentary sections (pseudowell 3 on the shelf and pseudowell 16 on the deep-water margin) were almost identical despite the areas having different subsidence histories (Fig. 4). This phenomenon can be explained by a higher heat flow in the marginal rift during lithospheric stretching and at the beginning of oceanic spreading than that of the intracontinental rift. At the same time, the modeling demonstrated a higher degree of source rock maturity in pseudowell 4 than that in pseudowell 14 despite the comparative thicknesses of their overlaying mantle. This can be explained by the dominating effect of an organic matter maturation in the vicinity of pseudowell 4 if compared to the thermal effect in the vicinity of pseudowell 14 within the same time period.

The performed numerical modeling enables us to assume that the sediments started to deposit on the lithosphere that had become β_0 times thinner. The duration of this initial thinning is not important in our modeling; it could occur from 5 to 20 Ma. It is important to note that the errors of 10–15 Ma in dating of when the sedimentation begun as well as the error of 100–300 m in determination of paleosea depths should not have a significant effect on the results of modeling.

The resulting amplitudes of presedimentary lithospheric stretching β_0 are depicted in Fig. 8*a* (curve 1). They reach

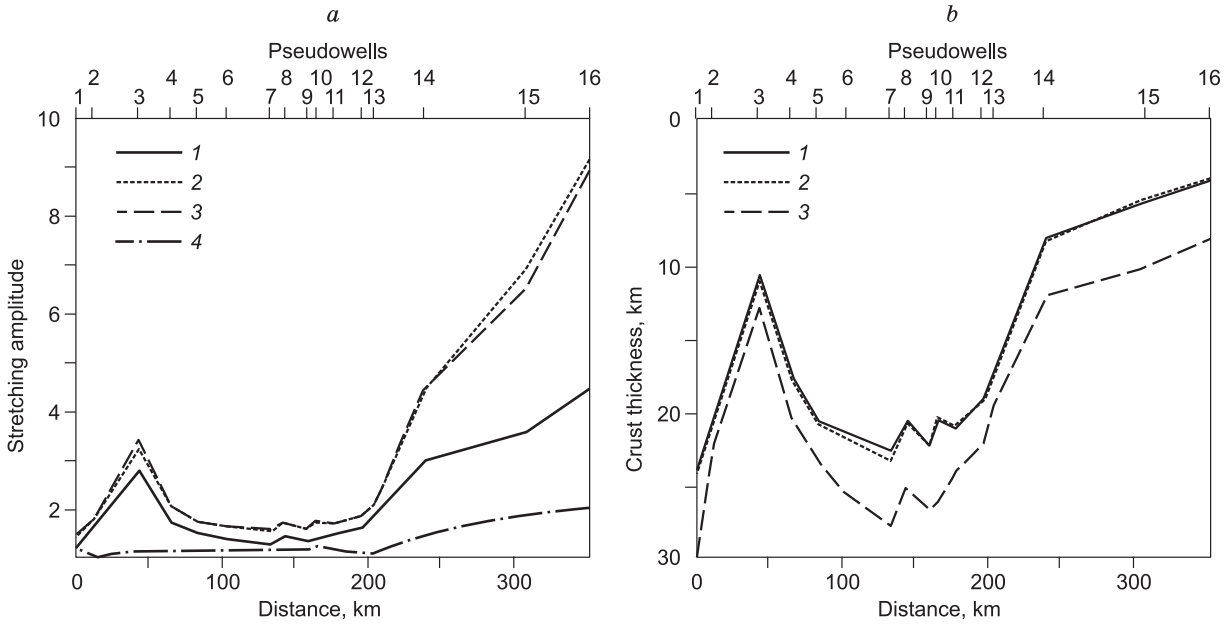

Fig. 8. Changes in the amplitudes of lithospheric stretching (*a*) and the thickness of the crystalline crust (*b*) along the modeled profile (Figs. 2, 3). *a*: *1*, stretching amplitude before the start of sedimentation (β_0); *2*, calculated summed stretching amplitude (β_{sum}); *3*, observed stretching amplitude (β_{observ}) obtained from gravity modeling (Fig. 2) as $36/H_{consol}$, where H_{consol} denotes the thickness of the crystalline crust; its value of 36 km was assumed as initial for unstretched crust that is typical for East Antarctica (Baranov et al., 2018); *4*, stretching amplitude during rift-related sedimentation (β_{12}); *b*: *1*, thickness of the crystalline crust obtained from density modeling (Fig. 2); *2*, thickness of the crystalline crust obtained from stretching amplitude modeling; *3*, thickness of the crystalline crust during the early stage of rifting before the start of sedimentation ($H_{0sed} = 36/\beta_0$, where β_0 is curve *1* in Fig. 8*a*).

the value of 2.8 in the central part of the intracontinental rift and of 4.5 in the marginal rift in the vicinity of the continent-ocean boundary. If we suggest that sedimentation started 270 Ma in the Lambert intracontinental rift and 170 Ma in the margin rift on the lithosphere with normal (unstretched) continental crust of 36 km thick, analysis of tectonic subsidence variations will give us the stretching amplitudes that are significantly less than those observed. In this case, the calculated thickness of the consolidated crust will be 2–3 times higher than its actual thickness (Galushkin et al., 2018). Our estimations have demonstrated that the stretching amplitude (β_0) before the start of deposition can significantly exceed the stretching amplitude during sedimentation (β_{12}).

CONCLUSIONS

The sedimentary basin of the Cooperation Sea is located on Antarctic continental margin in the southern part of the Indian Ocean and developed due to the rifting in East Gondwana followed by break up of India and Antarctica. The shelf part of the basin contains the northern termination of an intracontinental rift that adjoins the marginal rift. Based on seismic and gravity data, it has been confirmed that the thickness of the crystalline crust varies from 29 to 31 km in the rift flanks, to 11 km in the axial part of the intracontinental rift and to 8–5 km in the outer part of the marginal rift.

Seismic stratigraphy analysis has enabled us to determine the main seismic sequences and predict both their age and composition. Four sequences were identified for the intracontinental rift. They deposited during the periods of 270–210, 170–125, 125–34 and 34–0 Ma. In the marginal rift, 9 seismic sequences have been recognized, and they are interpreted to have formed during 170–125, 125–110, 110–90, 90–43, 43–34, 34–24, 24–14, 14–5, 5–0 Ma.

One-dimensional numerical modeling of the thermal regime, the basement subsidence and lithospheric stretching was performed along the profile crossing the basin from the shelf to the lower continental rise. The performed numerical modeling has demonstrated that in order to match the observed depths of the basement surface and the modern thicknesses of the crystalline crust, the rifting has to have a period of lithospheric stretching that preceded the subsidence and deposition of the sediments. Such a situation can be explained by the uplift of the crust during the early stage of rifting. The stretching reached its maximum in the axial parts of the intracontinental and marginal rifts, which resulted in the maximum thinning of the crust. In the depocenter of the intracontinental rift, the stretching amplitude was 2.8 before sedimentation began (before 270 Ma) and 1.16 afterwards. An extreme stretching has been observed in the outer part of the marginal rift. It reached 4.6 before the start of sedimentation (170 Ma) and 1.75 afterward. The total stretching amplitude in this area reached 8.

Our estimations of the stretching amplitudes during the sedimentary stage are based on the numerical modeling of the Cooperation Sea Basin; the history of the basement subsidence and changes in the rock temperatures. The modeling assumes the temperatures could reach higher orders (about 200 °C and higher) causing high degrees of organic matter maturation ($R^{o}_{Vt} > 2.00\%$) in the Triassic and Lower Jurassic rocks.

The study was performed with the support of the Russian Science Foundation (project No. 16-17-10139).

REFERENCES

Aleksashin, N.D., Laiba, A.A., 1993. Stratigraphy and litho-facial features of the Permian deposits of the western shore of the Beaver Lake (Prince Charles Mountains, East Antarctica) in Antarctica. Commission's Reports 31, 43–51.

Baer, A.J., 1981. Geotherms evolution of the lithosphere and plate tectonics. Tectonophysics 72 (3–4), 203–227.

Baranov, A., Tenzer, R., Bagherbandi, M., 2018. Combined gravimetric–seismic crustal model for Antarctica. Surv. Geophys. 39 (1), 23–56.

Barron, J., Larson, B. (Eds.), 1991. Proceedings of the Ocean Drilling Program, Scientific results Ocean Drilling Program, Vol. 119. College Station, TX.

Boillot, G., Froitzheim, N., 2001. Non-volcanic rifted margins, continental break-up and onset of seafloor spreading: some outstanding questions, in: Wilson, R.C.L., Whitmarsh, R.B., Taylor, B., Froitzheim, N. (Eds.), Non-Volcanic Rifting of Continental Margins: a Composition of Evidence from Land and Sea. Geol. Soc. London, Spec. Publ. 187, pp. 9–30.

Cooper, A.K., O'Brien, P.E., Richter, C. (Eds.), 2004. Proceedings of the Ocean Drilling Program, Scientific Results. Ocean Drilling Program, Vol. 188. College Station, TX. DOI:10.2973/odp.proc.sr.188.2004.

Florindo, F., Siegert, M. (Eds.), 2009. Antarctic Climate Evolution. Developments in Earth and Environmental Science, Vol. 8. Elsevier, Amsterdam.

Frakes, L.A., 1979. Climates throughout Geologic Time. Elsevier, New York.

Galushkin, Yu.I., 2007. Modeling of Sedimentary Basins and Estimations of Their Hydrocarbon Potential [in Russian]. Naychnyi Mir, Moscow.

Galushkin, Yu.I., 2016. Non-Standard Problems in Basin Modeling. Springer.

Galushkin, Yu.I., Leitchenkov, Yu.B., Guseva, Yu.B., Dubinin, E.P., 2018. The stretching amplitude and thermal regime of the lithosphere in the nonvolcanic passive margin of Antarctica in the Mawson Sea region. Izvestiya. Phys. Solid. Earth 54, 79–90.

Gupta, M.I., Sundar, A., Sharma, S.R., 1991. Heat flow and heat generation in the Archaean Dharwar cratons and implications for the Southern Indian Shield geotherm and lithospheric thickness. Tectonophysics 194 (1–2), 107–122.

Lawver, L.A., Gahagan, L.M., Coffin, M.F., 1992. The development of paleoseaways around Antarctica, in: Kennet, J.P., Barren, J. (Eds.), The Role of the Southern Ocean and Antarctica in Global Change: an Ocean Drilling Perspective. Antarctic Research Series, AGU, Vol. 56, pp. 7–30.

Leitchenkov, G.L., Guseva, Y.B., Gandyukhin, V.V., 2007. Cenozoic environmental changes along the East Antarctic continental margin inferred from regional seismic stratigraphy, in: Cooper, A.K., Barrett, P.J., Stagg, H., Storey, B., Stump, E., Wise, W. (Eds.), Antarctica: A Keystone in a Changing World. Proc. Xth Int. Symp. Antarctic Earth Sci. Natl. Acad. Press. Washington DC. DOI:10.3133/of2007-1047.srp005.

Leitchenkov, G.L., Guseva, Yu.B., Gandykhin, V.V., Gol', K., Ivanov, S.V., Golynskii, A.V., Kazankov, A.Yu., 2010. Tectonic development of Earth's crust and sedimentary mantle formation in the Antarctic part of the Indian Ocean (Cooperation Sea, Davis Sea, Kerguelen Plato), in: Leonov, Yu.G. (Ed.), Russian Studies under IPY Project 2007/2008. Lithospheric Composition and History [in Russian]. Paulsen, Moscow, pp. 9–38.

Leitchenkov, G.L., Guseva, Yu.B., Gandyukhin, V.V., Ivanov, S.V., Safonova, L.V., 2014. Structure of the Earth's crust and tectonic evolution history of the Southern Indian Ocean (Antarctica). Geotectonics 48, 5–23.

Leitchenkov, G.L., Belyatsky, B.V., Kaminsky, V.D., 2018. The age of rift-related basalts in East Antarctica. Dokl. Earth Sci. 478, 11–14.

Lisker, F., Brown, R., Fabel, D., 2003. Denudational and thermal history along a transect across the Lambert Graben, northern Prince Charles Mountains, Antarctica, derived from apatite fission track thermochronology. Tectonics 22 (5). DOI: 10.1029/2002TC001477.

Mangipudi, V.R., Goli, A., Desa, M., Tammisetti, R., Dewangan, P., 2014. Synthesis of deep multichannel seismic and high resolution sparker data: Implications for the geological environment of the Krishna–Godavari offshore, Eastern Continental Margin of India. Mar. Pet. Geol. 58, 339–355.

McKenzie, D., Jackson, J., Priestley, K., 2005. Thermal structure of oceanic and continental lithosphere. Earth Planet. Sci. Lett. 233 (3–4), 337–339.

Mikhalsky, E.V., Sheraton, J.W., 1993. Association of dolerite and lamprophyre dykes, Jetty Peninsula (Prince Charles Mountains, East Antarctica). Antarctic Sci. 5 (3), 297–307.

Parsons, B., Sclater, I.C., 1977. An analysis of the variation of ocean floor bathimetry and heat flow with age. J. Geophys. Res. 82 (5), 803–827.

Stagg, H.M.J., 1985. The structure and origin of Prydz Bay and Mac-Robertson Shelf, East Antarctica. Tectonophysics 114 (1–4), 315–340.

Touloukian, Y.S., Ho, C.Y., 1981. Physical Properties of Rocks and Minerals. McGrew-Hill, New York.

Truswell, E.M., Dettmann, M.E., O'Brien, P.E., 1999. Mesozoic palynofloras from the Mac. Robertson shelf, East Antarctica: geological and phytogeographic implications. Antarctic Sci. 11 (2), 239–255.

Ungerer, Ph., 1993. Modeling of petroleum generation and migration, in: Bordenave, M.L. (Ed.), Applied Petroleum Geochemistry. Technip, Paris, pp. 397–442.

Ungerer, Ph., Burrus, I., Doligez, B., Chenet, P., Bessis, F., 1990. Basin evaluation by integrated two-dimensional modeling of heat transfer, fluid flow, hydrocarbon generation, and migration. AAPG Bull. 74 (3), 309–335.

Welte, D.H., Horsfield, B., Baker, D.R. (Eds.), 1997. Petroleum and Basin Evolution. Springer-Verlag.

Wyllie, P.J., 1979. Magmas and volatile components. Am. Mineral. 64, 469–500.

Editorial responsibility: O.P. Polyansky